Human Molecular Genetics, 2020, Vol. 29, No. 5 705–715

doi: 10.1093/hmg/ddz233
Advance Access Publication Date: 10 October 2019
General Article

GENERAL ARTICLE

Nr2f1 heterozygous knockout mice recapitulate neurological phenotypes of Bosch-Boonstra-Schaaf optic atrophy syndrome and show impaired hippocampal synaptic plasticity

Chun-An Chen[1,2,†], Wei Wang[1,2,†], Steen E. Pedersen[3,4,5], Ayush Raman[2,6], Michelle L. Seymour[7], Fernanda R. Ruiz[7], Anping Xia[7], Meike E. van der Heijden[2,8], Li Wang[1,2], Jiani Yin[1,2], Joanna Lopez[1,2], Megan E. Rech[2], Richard A. Lewis[1,9], Samuel M. Wu[8,9], Zhandong Liu[2,10], Fred A. Pereira[7], Robia G. Pautler[3,4], Huda Y. Zoghbi[1,2,10,11,12] and Christian P. Schaaf[1,2,13,*]

[1]Department of Human and Molecular Genetics, Baylor College of Medicine, Houston, TX, USA, [2]Jan and Dan Duncan Neurological Research Institute, Texas Children's Hospital, Houston, TX, USA, [3]Department of Molecular Physiology and Biophysics-Cardiovascular Sciences Track, Baylor College of Medicine, Houston, TX, USA, [4]Department of Molecular Physiology and Biophysics, Baylor College of Medicine, Houston, TX, USA, [5]Department of Physiology and Biochemistry, Ross University School of Medicine, Portsmouth, Commonwealth of Dominica, [6]Graduate Program in Quantitative and Computational Biosciences, Baylor College of Medicine, Houston, TX, USA, [7]Huffington Center on Aging and Department of Molecular and Cellular Biology, Baylor College of Medicine, Houston, TX, USA, [8]Department of Neuroscience, Baylor College of Medicine, Houston, TX, USA, [9]Department of Ophthalmology, Baylor College of Medicine, Houston, TX, USA, [10]Department of Pediatrics, Baylor College of Medicine, Houston, TX, USA, [11]Program in Developmental Biology, Baylor College of Medicine, Houston, TX, USA, [12]Howard Hughes Medical Institute, Baylor College of Medicine, Houston, TX, USA, and [13]Institute of Human Genetics, Heidelberg University, Heidelberg, Germany

*To whom correspondence should be addressed at: Institute of Human Genetics, University Hospital Heidelberg, Im Neuenheimer Feld 366, 69120 Heidelberg, Germany. Tel: +49-6221-565151; Fax: +49-6221-565155; Email: schaaf@bcm.edu

Abstract

Bosch-Boonstra-Schaaf optic atrophy syndrome (BBSOAS) has been identified as an autosomal-dominant disorder characterized by a complex neurological phenotype, with high prevalence of intellectual disability and optic nerve atrophy/hypoplasia. The syndrome is caused by loss-of-function mutations in *NR2F1*, which encodes a highly conserved nuclear receptor that serves as a transcriptional regulator. Previous investigations to understand the protein's role in neurodevelopment have mostly used mouse models with constitutive and tissue-specific homozygous knockout of *Nr2f1*.

[†]These authors contributed equally to this work

Received: July 24, 2019. **Revised:** September 17, 2019. **Accepted:** September 23, 2019

In order to represent the human disease more accurately, which is caused by heterozygous *NR2F1* mutations, we investigated a heterozygous knockout mouse model and found that this model recapitulates some of the neurological phenotypes of BBSOAS, including altered learning/memory, hearing defects, neonatal hypotonia and decreased hippocampal volume. The mice showed altered fear memory, and further electrophysiological investigation in hippocampal slices revealed significantly reduced long-term potentiation and long-term depression. These results suggest that a deficit or alteration in hippocampal synaptic plasticity may contribute to the intellectual disability frequently seen in BBSOAS. RNA-sequencing (RNA-Seq) analysis revealed significant differential gene expression in the adult *Nr2f1*$^{+/-}$ hippocampus, including the up-regulation of multiple matrix metalloproteases, which are known to be critical for the development and the plasticity of the nervous system. Taken together, our studies highlight the important role of *Nr2f1* in neurodevelopment. The discovery of impaired hippocampal synaptic plasticity in the heterozygous mouse model sheds light on the pathophysiology of altered memory and cognitive function in BBSOAS.

Introduction

Bosch-Boonstra-Schaaf optic atrophy syndrome (BBSOAS [MIM: 615722]) has been identified recently as an autosomal-dominant disorder characterized by a complex neurological phenotype, including optic nerve atrophy/hypoplasia, developmental delay, intellectual disability, hypotonia, oromotor dysfunction, thin corpus callosum, seizures, autism spectrum disorder, attention deficit hyperactivity disorder and hearing impairment, each with variable penetrance (1–5). BBSOAS is caused by mutations in *NR2F1* (nuclear receptor subfamily 2 group F member 1). To date, ~40 individuals with *NR2F1* pathogenic variants have been reported. *NR2F1* encodes a highly conserved nuclear hormone receptor and transcriptional regulator. Human NR2F1 shares more than 99% amino acid sequence identity with its mouse homologue. Previous studies in multiple *Nr2f1* knockout mouse models revealed its functions in neurodevelopment, among which are cortical patterning (6), eye development (7,8) and neurogenesis (9). While most studies have focused on constitutive homozygous knockout (perinatal lethality) (10) or tissue-specific homozygous knockout animals (6,7,9), all reported human individuals diagnosed with BBSOAS have heterozygous pathogenic *NR2F1* variants. To avoid the perinatal lethality and, more importantly, to model the human disease better, we investigated an *Nr2f1* heterozygous knockout mouse model (*Nr2f1*$^{+/-}$), using a battery of behavioral tests, electrophysiological studies and brain magnetic resonance imaging (MRI). We also performed RNA sequencing (RNA-Seq) to investigate the differential gene expression in *Nr2f1*$^{+/-}$ mice. We found that this mouse model recapitulates multiple neurological phenotypes of BBSOAS, providing insight into the affected tissues and the alterations leading to the disease.

Results

Nr2f1$^{+/-}$ mice do not show decreased visual contrast sensitivity

Nr2f1$^{+/-}$ mice used in this study had been generated previously (10). The knockout allele deletes the entire DNA-binding domain and two-thirds of the ligand-binding domain. The knockout allele is considered as a null instead of a dominant-negative mutant, as no *Nr2f1* transcripts were detected in *Nr2f1*$^{-/-}$ embryos (10). We first checked whether *Nr2f1*$^{+/-}$ mice display visual impairment, given that optic nerve atrophy/hypoplasia in human patients with BBSOAS results in various degrees of vision loss. The optokinetic reflexes are reflexive head and eye movements elicited by a visual stimulus moving along a horizontal direction and function to stabilize an image on the retina. This visually guided behavior relies on the ability of the retina to detect a contrast difference between the darker and lighter bars in a stimulus (Fig. 1A) (11,12). No significant difference in contrast sensitivity between 8-week-old *Nr2f1*$^{+/-}$ and wild-type mice was found with the optokinetic reflex test (Fig. 1B). These data suggested that *Nr2f1*$^{+/-}$ mice do not have significantly decreased visual performance.

Nr2f1$^{+/-}$ mice display hearing defects and neonatal hypotonia

Because some BBSOAS patients have hearing impairment, we measured hearing ability in *Nr2f1*$^{+/-}$ mice with the auditory brainstem response (ABR), which is used widely in infants and lab animals to assess hearing defects resulting from neurological abnormalities of the auditory nerves and the auditory pathway (13). Auditory thresholds were determined by decreasing the sound intensity of each stimulus in 5 dB steps (90 to 10 dB). In comparison with wild-type littermates, the 9-week-old *Nr2f1*$^{+/-}$ mice showed an ABR threshold increase at low frequency stimulation (4 and 8 kHz) (Fig. 1C). The 18-week-old *Nr2f1*$^{+/-}$ mice showed significantly increased ABR thresholds at the stimulation frequency of 8 and 16 kHz (Fig. 1D). However, the histology and immunofluorescence staining in the *Nr2f1*$^{+/-}$ mice showed no gross abnormalities in the organ of Corti at embryonic day 18 (E18) and postnatal day 2 (p2) (Supplementary Material, Figure S1 (A)–S1 (D)). Distortion product otoacoustic emission (DPOAE) test was used to assess the function of outer hair cells in p20 mice. We did not see a significant change in the DPOAE threshold between *Nr2f1*$^{+/-}$ and wild-type mice (Supplementary Material, Figure S1 (E)). These data suggest that *Nr2f1*$^{+/-}$ mice recapitulate the hearing defects of BBSOAS patients.

Given that ~75% of BBSOAS patients have hypotonia and ~60% of BBSOAS patients have a history of feeding difficulties (a manifestation of decreased muscle tone in humans at a young age that usually resolves later in life), we tested whether *Nr2f1*$^{+/-}$ mice have hypotonia by performing the surface-righting test (14,15). Postnatal day 6 (p6) pups were placed on a flat surface on their back with all paws facing up in the air. The latency to flipping over onto their stomach with all paws touching the surface was measured. Longer latency is expected in hypotonic pups. As shown in Figure 1E, a surface-righting test on p6 *Nr2f1*$^{+/-}$ and wild-type pups showed a statistically significant difference, with *Nr2f1*$^{+/-}$ pups taking more time to right themselves in contrast to wild-type littermates. These data suggest that *Nr2f1*$^{+/-}$ pups have neonatal hypotonia. Notably, the body weight of p6 *Nr2f1*$^{+/-}$ pups is significantly less than the wild-type pups, which is likely caused by feeding difficulties resulting from decreased muscle tone (Fig. 1F). The grip strength assay measures the maximum force of the mice

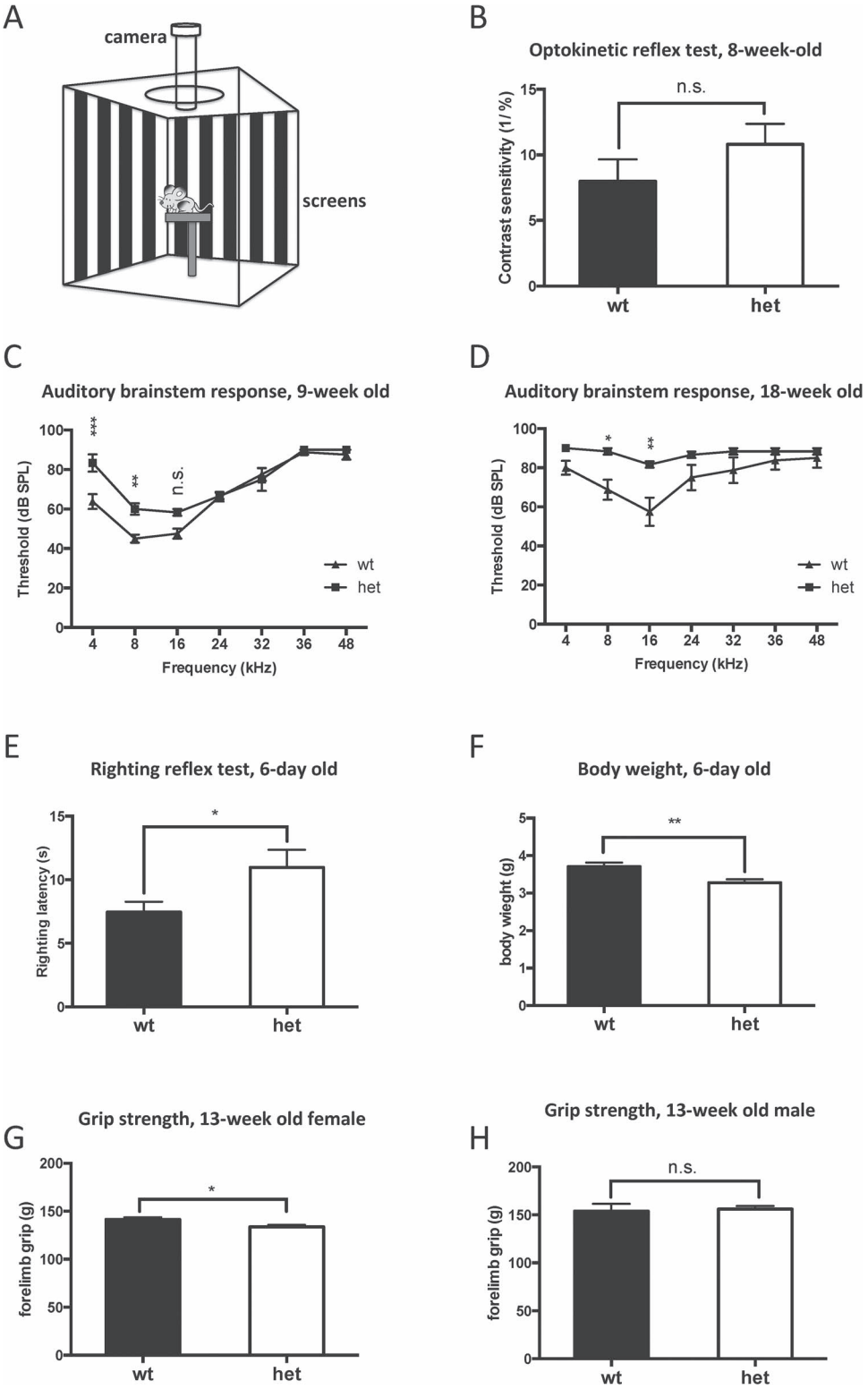

Figure 1. *Nr2f1*$^{+/-}$ mice have hearing defects and neonatal hypotonia. (**A**) Illustration of optokinetic reflex test. (**B**) Contrast sensitivity of 8-week-old mice in the optokinetic reflex test, as an indication of visual performance. $N = 10$. (**C, D**) The hearing ability was evaluated by the ABR in 9-week-old mice (C) and 18-week-old mice (D). $N = 3$–4. (**E**) Latency of p6 pups to flip from their back onto their stomach with all paws on the surface in the righting reflex test. Long latency indicates hypotonia. $N = 19$–21. (**F**) Body weight of p6 pups. $N = 19$–21. (**G**) Maximum force of the forelimb pulling by 13-week-old female mice, as an indication of muscle strength. $N = 13$–15. (**H**) Maximum force of the forelimb pulling by 13-week-old male mice, as an indication of muscle strength. $N = 10$–18. Data are shown as mean ± standard error of mean. n.s. not significant, $^{*}P < 0.05$, $^{**}P < 0.01$, $^{***}P < 0.001$.

forelimbs grabbing a bar. This test assesses muscle strength and tone in adult mice (16). Grip strength assay on 13-week-old female *Nr2f1*$^{+/-}$ mice showed a small, but significant decrease in forelimb grip strength in contrast with that of wild-type female mice (Fig. 1G). However, we found no significant difference in grip strength between male *Nr2f1*$^{+/-}$ and male wild-type littermates (Fig. 1H). The data of the grip strength assay are presented individually for each sex, as the body weight of male mice is significantly heavier than that of female mice. There was no significant body weight difference between female *Nr2f1*$^{+/-}$ and female wild-type littermates when the assay was performed (Supplementary Material, Figure S2 (F)). Taken together, our data suggest that *Nr2f1*$^{+/-}$ mice have neonatal hypotonia.

Some BBSOAS patients also manifest neurobehavioral or psychiatric features, such as autism spectrum disorder, attention deficit hyperactivity disorder/attention deficit disorder and repetitive behaviors. To assess the corresponding behavioral traits in mice, we performed the elevated plus maze test and the light dark box test for anxiety-like behaviors (Supplementary Material, Figure S2 (A) and S2 (B)); the marble burying assay for repetitive digging behaviors (Supplementary Material, Figure S2(C)) and the 3-chamber interaction assay for sociability (Supplementary Material, Figure S2 (D)). Other tests conducted with the mice included the accelerating rotarod test for motor learning and coordination (Supplementary Material, Figure S2 (E)), and the acoustic startle response test followed by prepulse inhibition testing for schizophrenia-associated behavior (Supplementary Material, Figure S2 (G) and S2 (H)). In short, *Nr2f1*$^{+/-}$ mice behaved largely normal in all these tests in contrast to wild-type littermates, except that *Nr2f1*$^{+/-}$ mice showed decreased acoustic startle response (Supplementary Material, Figure S2 (G)), which may be resulting from decreased muscle tone or hearing deficits.

Nr2f1$^{+/-}$ mice have decreased hippocampal volume and display altered fear memory

Given that structural brain anomalies are reported in a subset of BBSOAS patients, we examined the brain structure of adult *Nr2f1*$^{+/-}$ mice using MRI. While the general brain morphology and the volume of the whole brain are normal, MRI volumetric analysis indicated that *Nr2f1*$^{+/-}$ mice have a smaller hippocampal volume and increased volume in other brain regions such as neocortex, caudate and putamen (Fig. 2A). Quantification of neuronal cell density in the somatosensory cortex and striatum by counting the NeuN-positive cells showed no significant difference between *Nr2f1*$^{+/-}$ mice and wild-type littermates (Supplementary Material, Figure S3 (A) and S3 (B)), suggesting that *Nr2f1*$^{+/-}$ mice have an increased total number of neuronal cells in these brain regions without altering cell density. Given the role of the hippocampus in learning and memory, and the high prevalence of mild to moderate intellectual disability in patients with BBSOAS, we investigated whether *Nr2f1*$^{+/-}$ mice have learning/memory deficits using two different behavioral tests: the contextual fear conditioning test and the spontaneous alternation Y-maze test. In the contextual fear conditioning test, the mice were trained on Day 0 to associate the chamber with an electric foot shock. Fear memory response was evaluated the following days by scoring the freezing time when the mice were placed in the same chamber (Fig. 2C). On Day 1 (24 h after training), *Nr2f1*$^{+/-}$ and wild-type littermates froze for similar amounts of time, suggesting that *Nr2f1*$^{+/-}$ mice do not have an impairment in contextual fear learning (Fig. 2B). The extinction of fear memory was achieved by repeated exposure of the mice to the same chamber once a day for 5 min each day without foot shock. We found that *Nr2f1*$^{+/-}$ mice showed an alteration in memory extinction on Day 2, as they spent significantly more time freezing in contrast to their wild-type littermates. A similar trend was also observed at Day 3, but without statistical significance (Fig. 2B). This suggests a possible deficit or alteration in fear memory extinction in *Nr2f1*$^{+/-}$ mice, which is particularly interesting in the context of reports of prolonged memory in human BBSOAS patients (Dr. Schaaf, personal reports). We also evaluated the spatial working memory in *Nr2f1*$^{+/-}$ mice by performing the spontaneous alternation Y-maze test, which makes use of the tendency of mice to explore alternate maze arms on successive trials (Fig. 2D). No significant difference was found between *Nr2f1*$^{+/-}$ mice and wild-type littermates (Fig. 2E). Taken together, these data suggest that *Nr2f1*$^{+/-}$ mice display altered fear memory, while spatial working memory appeared to be normal.

Nr2f1$^{+/-}$ mice show impaired synaptic plasticity in the hippocampus

We investigated the mechanisms underlying the altered fear memory by electrophysiological studies, testing synaptic transmission and plasticity in the hippocampus. In acute hippocampal slices obtained from adult *Nr2f1*$^{+/-}$ mice, we studied the Schaffer collateral synapses in CA1. The paired-pulse ratio showed no significant changes in pre- and postsynaptic transmission when comparing *Nr2f1*$^{+/-}$ mice and wild-type littermates (Fig. 3A). To investigate the synaptic plasticity in the hippocampus of *Nr2f1*$^{+/-}$ mice, we measured long-term potentiation (LTP) and long-term depression (LTD), both of which have been studied extensively and are believed to represent cellular correlates of learning and memory (17). LTP and LTD affect neuronal synaptic plasticity by increasing and decreasing synaptic strength, respectively. While LTP was induced in the wild-type animals by a standard stimulation protocol (two trains of 100 Hz for 1 s with a 20 s inter-train intervals), LTP was largely absent in *Nr2f1*$^{+/-}$ mice (Fig. 3B and C). LTD, the activity-dependent reduction in the efficacy of neuronal synapses was significantly impaired in *Nr2f1*$^{+/-}$ mice. The hippocampal slices of *Nr2f1*$^{+/-}$ mice failed to maintain the LTD, which had been induced by low-frequency stimulation (200 ms paired pulse interval, 900 stimuli and 1 Hz inter-pair interval) (Fig. 3D and E). The dendritic spine morphology and the overall spine density of the primary hippocampal neuronal culture derived from *Nr2f1*$^{+/-}$ mice are not significantly different from those of wild type littermates (Supplementary Material, Figure S3 (C)).

To study the molecular changes that might lead to altered fear memory and deficits in hippocampal LTP and LTD, we performed RNA-Seq to compare gene expression in the hippocampus of adult *Nr2f1*$^{+/-}$ and wild-type mice. Expression of 1153 genes differed significantly (876 and 277 genes are up-regulated and down-regulated in *Nr2f1*$^{+/-}$ hippocampus, respectively) (Fig. 3(F) and Supplementary Material, Table S2). Multiple matrix metalloproteases (MMPs) were found to be up-regulated in the *Nr2f1*$^{+/-}$ hippocampus. MMPs are critical for the development and the plasticity of the nervous system (18). We validated the up-regulation of *Mmp2*, *Mmp15* and *Hspg2* in the MMP pathway by quantitative PCR (Fig. 3G). Analyzing the RNA-Seq data set based on an overlap enrichment of the down-regulated genes using the Intellectual and Developmental Disability (IDD) genes available from literature (method similar to Pohodich *et al.* (19)) detected no significant findings.

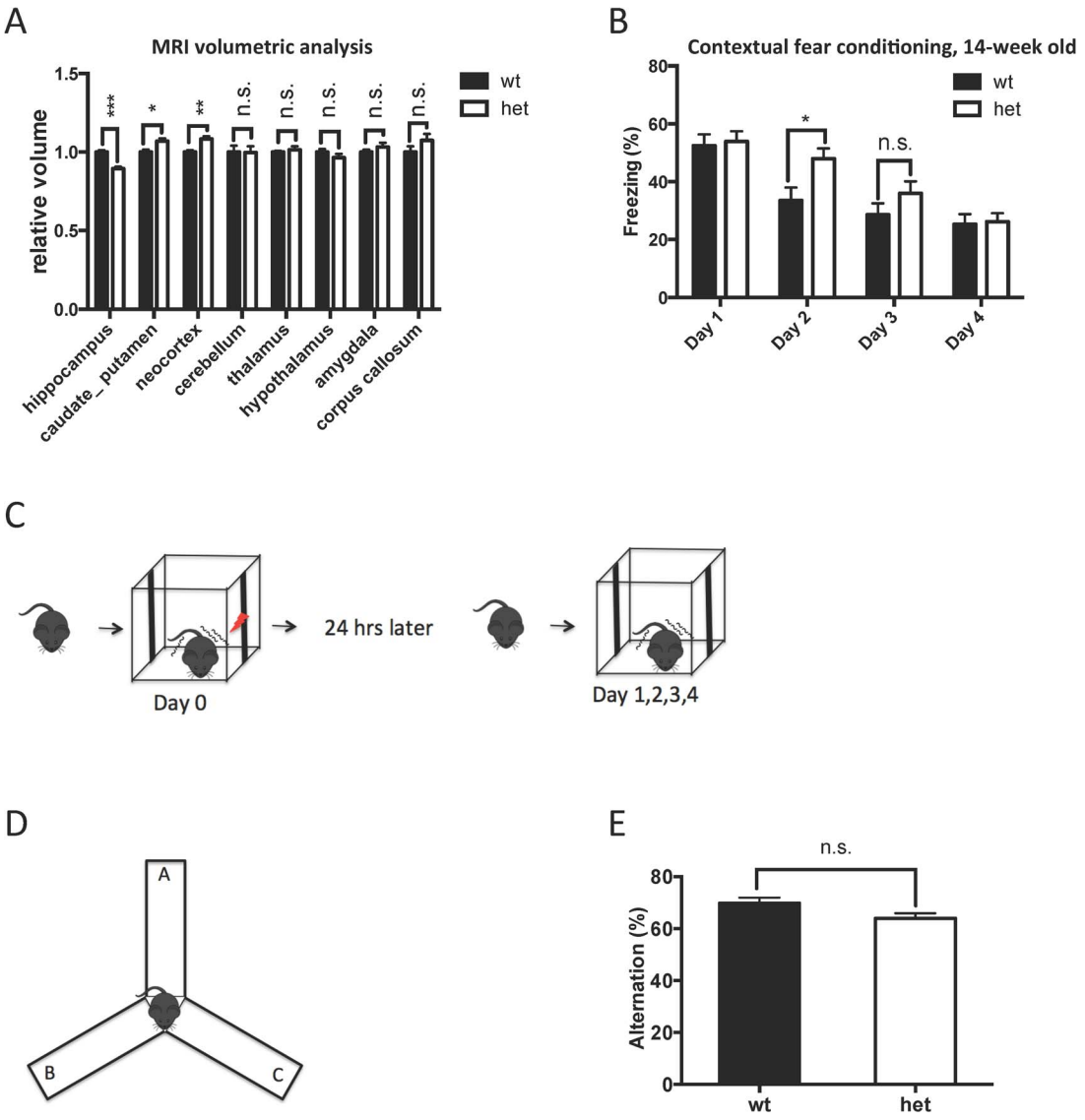

Figure 2. *Nr2f1*$^{+/-}$ mice have decreased hippocampal volume and display altered fear memory. (**A**) MRI volumetric analysis of different brain regions. $N = 5$. (**B**) Conditioned fear testing. Graphs indicate time spent freezing in the shock chamber. Fear memory retention was evaluated from Day 1 to Day 4 daily, when mice were placed in the same chamber for 5 min without tone or foot stimuli. $N = 25–30$. (**C**) Illustration of contextual fear conditioning and fear memory retention test. (**D**) Illustration of spontaneous alternation Y-maze test. (**E**) The alternation score in spontaneous alternation Y-maze, as an indication of spatial working memory. $N = 32–35$. Data are shown as mean ± standard error of mean. n.s. not significant, $^{*}P < 0.05$, $^{**}P < 0.01$, $^{***}P < 0.001$.

Discussion

Individuals with BBSOAS manifest an array of neurological and behavioral features, which may be in part a reflection of NR2F1's critical role as a transcriptional regulator during neurodevelopment. Here we report a mouse model for BBSOAS and provide a characterization of neuronal and behavioral phenotypes, using brain MRI, electrophysiological studies and behavioral investigation. Hippocampus-related phenotypes are a focus in our study, as intellectual disability is one of the most prominent and most highly penetrant features of BBSOAS. Reduced hippocampal volumes have been reported in schizophrenia (20), post-traumatic stress disorder (21), depression (22) and intellectual disability-associated genetic disorders (23,24). Previous studies of a tissue-specific knockout of mouse *Nr2f1* in the neocortex and hippocampus showed about 50% reduction of overall hippocampal volume (25). However, such dramatic reduction was neither detected in BBSOAS patients nor in our heterozygous mouse model (10% reduction), which demonstrates the importance of gene dosage in this translational disease model. Reduction of hippocampal volume has not been reported in BBSOAS patients, which may be based on lack of sensitivity of clinical MR imaging or lack of such targeted analysis. Future investigation of hippocampal volume and structure in BBSOAS patients should be considered, as even small developmental variations in hippocampal volume may impact cognitive function, as documented in 22q11.2 deletion syndrome (24,26), for example. Spatial memory defects in the water maze test have been reported in neocortical- and hippocampal-knockout models of *Nr2f1* (25). Here, we showed that loss of one copy of *Nr2f1* is sufficient to cause altered fear memory, likely resulting from the impairment in hippocampal LTD. LTD and LTP are coordinated processes to maintain the homeostasis of synaptic plasticity by modulating synaptic strength. LTD is necessary for behavioral flexibility (27),

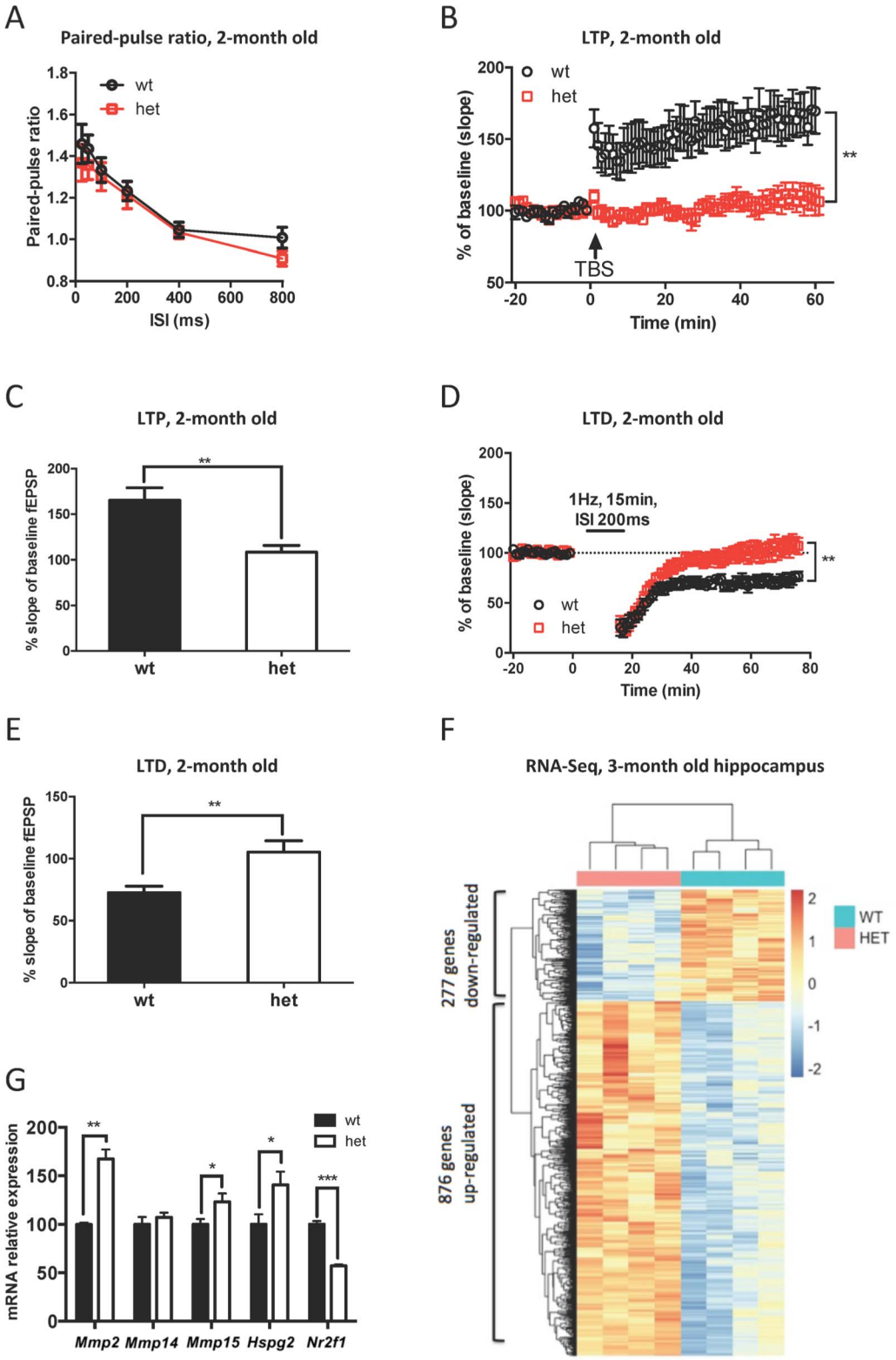

Figure 3. Impaired synaptic plasticity in the hippocampus of *Nr2f1*$^{+/-}$ mice. (**A**) No significant alterations of paired-pulse ratio (PPR) of fEPSPs between *Nr2f1*$^{+/-}$ mice and wild type littermates. $N = 14$. (**B**) Impairment of theta-burst stimulation (TBS)-induced LTP in slices from the *Nr2f1*$^{+/-}$ hippocampus. $N = 13$. (**C**) Quantification of the fEPSP slope 50–60 min after TBS stimulation as shown in (B). (**D**) Impairment of low-frequency stimulation-induced LTD in slice from the *Nr2f1*$^{+/-}$ hippocampus. $N = 8$. (**E**) Quantification of the fEPSP slope 65–75 min after low-frequency stimulation as shown in (D). (**F**) Heatmap of differential gene expressions in the hippocampus of 3-month-old *Nr2f1*$^{+/-}$ mice. $N = 4$. Clustering of the heatmap is based on the adjusted $P < 0.05$. (**G**) Validation of the RNA-Seq results (up-regulation of the matrix metalloprotease pathway) by quantitative real-time polymerase chain reaction. $N = 3$. Data are shown as mean ± standard error of mean. $^{*}P < 0.05$, $^{**}P < 0.01$, $^{***}P < 0.001$.

as LTD impairments in mice have been reported to disrupt fear memory extinction (28) and the reversal learning task (29), in which mice learn to adapt their behavior when the reward values or punishment are reversed from previous conditions. Interestingly, although most BBSOAS patients are diagnosed with mild to moderate intellectual disability by intelligent quotient testing, many of them have been reported to have extraordinary long-term memory. For example, the individual (Individual 6 in Bosch *et al*. (1)) with a *de novo* missense variant, c.335G>A (p.Arg112Lys), speaks two languages fluently and possesses an exceptional ability to remember dates of birth years later while having an IQ of 52. A cohort of ~50 individuals with BBSOAS will be presented in another report (M.R. *et al*., in submission), which shows that ~79% of the patients have unusually good long-term memory.

We performed ophthalmoscopic examination in *Nr2f1*$^{+/-}$ mice to check for optic nerve defects in addition to the optokinetic reflex testing, which evaluates the entire visual pathway, including retina, diencephalon, midbrain, pons and dorsal medulla (30). We did not find a significant difference between *Nr2f1*$^{+/-}$ and wild-type littermates in either test. This could be explained by the functional redundancy between *Nr2f1* and its paralog, *Nr2f2*. An eye-specific double knockout of *Nr2f1* and *Nr2f2* in mice leads to major eye abnormalities, but does not do so in eye-specific single knockout of *Nr2f1* (7). Interestingly, Bertacchi *et al*. recently showed that another heterozygous knockout mouse model displays multiple ocular abnormalities, including optic disk malformations, reduced optic axonal conduction velocity and associative visual learning deficits (8). In their associative visual learning behavioral assay, while the reported heterozygous knockout mice were able to reach the selection criteria (to associate between pressing a lever and obtaining a food pellet) as the wild-type mice during the preliminary training in a well-illuminated environment, the heterozygous knockout mice showed a deficit in associating the dim visual cue with the operant task (obtaining a food pellet by pressing the lever only during the 'light on' period but not 'light off' period in a light on/light off protocol). In agreement with our result, this experiment may suggest that the *Nr2f1* heterozygous knockout mouse models do not manifest dramatic vision impairment, at least in the well-illuminated environment. Regarding the ocular abnormalities, Bertacchi *et al*. proposed that the discrepancy between the eye-specific single knockout of *Nr2f1* (7) and their constitutive heterozygous knockout mouse model may be explained by the mouse model difference and/or the efficiency and timing of the conditional knockout mice. Additional investigation is needed to find out the underlying cause of the difference.

Several behavioral phenotypes observed in individuals with BBSOAS were not reproduced in this mouse model of heterozygous *Nr2f1* deletion. This may be explained, in part, by the higher sensitivity of detecting such alterations in humans. Additionally, it should be noted that individuals with point mutations in the DNA-binding domain of NR2F1 have a more severe phenotype in contrast to individuals with heterozygous deletion of the entire gene based on a dominant-negative effect (3). The same may be true in mice. Another loss-of-function *Nr2f1* mouse model, with conditional knockout of *Nr2f1* in neocortical and hippocampal neurons, has also been assessed for repetitive and anxiety-like behaviors. No significant repetitive behaviors in the marble burying assay and the nestlet shredding test were found (31). The same model showed no anxiety-like behaviors in the elevated plus maze test (25). However, decreased anxiety-like behaviors were described in another report using the same mouse model. There, elevated plus maze and dark-light tests were used, although no changes in anxiety were observed in the open-field assay in the same study (31).

Several reports suggest a possible genotype–phenotype correlation in BBSOAS (3,32), with missense variants in the DNA-binding domain leading to a more severe phenotype in contrast with the ones in the ligand-binding domain or whole gene deletions. A dominant negative effect was proposed to be the likely cause of the phenotypic severity in BBSOAS patients carrying the DNA-binding domain variants (3). Given that the heterozygous knockout mouse model in this study already manifests multiple neurological defects, it would be interesting to see whether knock-in mouse models bearing the DNA-binding domain variants may manifest a more pronounced phenotype in contrast to *Nr2f1*$^{+/-}$ mice.

Conclusions

We characterized a heterozygous knockout *Nr2f1* mouse model as a BBSOAS disease animal model, which recapitulates multiple neurological phenotypes. We showed that loss of one copy of *Nr2f1* leads to decreased hippocampal volume, altered learning/memory, hearing defects and neonatal hypotonia. A summary of phenotypes observed in this study and the biomedical literature is presented in Supplementary Materials, Table S1.

The discovery of impaired hippocampal synaptic plasticity in the mouse model sheds light on the pathophysiology of cognitive deficits and memory phenotypes in BBSOAS patients. Future studies should further investigate the direct targets of Nr2f1 and the molecular and cellular pathways that are part of the memory-related deficits. Human studies including high-resolution MR imaging are needed to explore long-term memory in BBSOAS and further refine hippocampal phenotypes.

Materials and Methods

Measurement of optokinetic reflexes (OKR)

We tested visually guided behavior in 8-week-old heterozygote and wild-type mice to determine whether visual function was affected in *Nr2f1*$^{+/-}$ mice. We choose to test contrast sensitivity using OKR as these reflexes are independent of cortical function and have been successfully used to detect abnormal retinal function in a wide range of mouse models (11,12,33,34). OKRs are the involuntary moments of mice's heads in the (temporal to nasal) direction of a moving contrast gradient. The contrast gradient (%) that is sufficient to evoke such a response half of the time is defined as the contrast sensitivity of the eye. We tested contrast sensitivities using a custom-built OKR set up previously described (11,12). In short, mice were exposed to 100 moving gradients (50 leftward, 50 rightward) that were displayed as a virtual cylinder displayed on four screens surrounding the mouse. A custom written protocol in MATLAB controlled gradient contrast and direction using a Bayesian one-step-ahead search, based on a prior protocol from extended previous testing of C57BL/6 mice. A trained observer chose the expected direction of the stimulus based on the mouse' head movements after each trial. During the experiment, the observer was masked to direction and contrast of the stimuli, as well as the genotype of the mouse. Each mouse was adapted to the behavior room for 2 h prior to testing, and all tests were performed in the dark to minimize effects of light adaption to behavioral responses. The mean photopic light intensity was 0.87 log10 cd/m^2, and relative intensities ranged approximately 2 log units from peak to peak

at highest contrast. Data are shown as mean ± standard error of mean and analyzed by unpaired t-test.

Auditory brainstem response

ABRs were measured as previously described (35). Briefly, 2-month-old or 4-month-old mice were anesthetized using an intraperitoneal injection of ketamine (100 mg/kg) and xylazine (10 mg/kg). Normal body temperature was maintained throughout the procedure by placing the mice on a heating pad. Pure tone stimuli from 4 to 48 kHz (ABRs) were generated using Tucker Davis Technologies System 3 digital signal processing hardware and software (Tucker Davis Technologies, Alachua, FL, USA), and the intensity of the tone stimuli was calibrated using a type 4938 1/4″ pressure-field calibration microphone (Brüel and Kjær, Nærum, Denmark). ABR signals were recorded with subcutaneous needle electrodes inserted at the vertex of the scalp, the postauricular region (reference) and the back leg (ground). Auditory thresholds were determined by decreasing the sound intensity of each stimulus in 5 dB steps (90 to 10 dB) until the lowest sound intensity with reproducible and recognizable ABR waveforms was reached. Data are shown as mean ± standard error of mean and analyzed by two-way ANOVA with repeated measurement with Bonferroni's post hoc analysis.

Righting reflex test

The latency to righting is commonly used to assess the basic motor coordination and hypotonia in mice at early developmental ages (14). p6 pups were placed on a flat surface on their back with all paws facing up in the air. The latency to flipping over onto its stomach with all paws touching the surface was recorded. The test was repeated four times, and the average time to right was calculated. Data are shown as mean ± standard error of mean and analyzed by unpaired t-test.

Grip strength

Grip strength was tested by holding 13-week-old mice by the tail and allowing them to grasp the middle of a bar (Chatillon-Ametek) with both forepaws. Mice were pulled away from the bar until they released the bar. Each mouse completed three pulls, and the maximum force from each pull was averaged. Data are shown as mean ± standard error of mean and analyzed by unpaired t-test.

MRI of the mouse brain

Eight-month-old *Nr2f1*$^{+/-}$ or wild-type littermates were transcardially perfused with heparinized 1× PBS followed by 4% PFA fixation. The skin, muscle, ear, nose tip and lower jaw were removed to expose the skull. The head was then fixed in 4% PFA overnight at 4°C. The head was then transferred to 0.01% sodium azide in 1× PBS for 7 days at 4°C followed by a final transferring to 5 mM gadopentetate dimeglumine and 0.01% sodium azide in 1× PBS. Mouse brains were then scanned by MRI using a diffusion tensor imaging (DTI) protocol to determine directional water diffusion within the brain. The DTI scans were analyzed for fractional anisotropy as a metric for the presence of white matter. Alignment and automated segmentation of the brains permitted quantitative comparison of white matter density in various brain regions, as well as determination of volume changes. Whole-brain voxel-by-voxel statistical analysis further revealed regions of difference.

Contextual fear conditioning and fear memory retention

Contextual fear conditioning was used to evaluate the learning and memory formation in 14-week-old mice as previously described with few modifications (36,37). The mice were trained at Day 0 in a chamber with a grid floor that could deliver an electric shock (Med Associates, Inc.). Each mouse was habituated in the chamber for 2 min, after which a tone (30 s, 5 kHz, 85 dB) coincided with a scrambled foot shock (2 s, 0.72 mA). The tone/foot-shock stimuli were repeated 2 min later. The mice were then returned to the home cage. Fear memory retention was evaluated on Day 1 to Day 4 daily. At each time point, mice were placed in the same chamber for 5 min without tone or foot stimuli. The freezing of the mice was recorded and scored automatically by ANY-maze (Stoelting). Data are shown as mean ± standard error of mean and were analyzed by two-way ANOVA with Bonferroni's post hoc analysis.

Continuous spontaneous alternation Y-maze

The spontaneous alternation Y-maze was used to evaluate the spatial working memory in 14-week-old mice as previously described with few modifications (38). The mice were placed in the center area of the Y-maze and allowed to freely explore the maze for 5 min. The sequence of arms explored by the mice was recorded by ANY-maze (Stoelting). The alternation score was calculated by (number of alternations)/(total arm entries minus two) (39). Data are shown as mean ± standard error of mean and analyzed by unpaired t-test.

Electrophysiology

Two-month old mice were anesthetized by isoflurane inhalation and decapitated. Transverse hippocampal slices (400 μm) were prepared in chilled cutting solution containing (in mM): 220 mM sucrose, 2.5 mM KCl, 0.5 mM $CaCl_2$, 7 mM $MgCl_2$, 1.25 mM NaH_2PO_4, 25 mM $NaHCO_3$ and 7 mM D-glucose. Slices were recovered in artificial cerebrospinal fluid (ACSF) containing 125 mM NaCl, 2.5 mM KCl, 2 mM $CaCl_2$, 1 mM $MgCl_2$, 1.25 mM NaH_2PO_4, 25 mM $NaHCO_3$ and 14.83 mM D-glucose for 30 min at 37°C and then incubated at room temperature. Field excitatory postsynaptic potentials (fEPSPs) were recorded from Schaffer collaterals of CA1, and a bipolar tungsten stimulation electrode (WPI) was placed in the middle region of the stratum radiatum to stimulate the Schaffer collaterals every 20 s. The recording pipettes were filled with the 2 M NaCl (1–2 MΩ), and their distance to the stimulating electrode were kept constant (~300 μm). Input/output (I/O) curves were generated using incremental stimulus intensities and were used to assess baseline synaptic transmission. For LTP and LTD experiments, stable baseline fEPSPs were recorded for 20 min at an intensity that induced ~40% of the maximal evoked response. LTP was induced by high-frequency stimulation consisting of two trains of 100 Hz for 1 s with 20 s inter-train intervals. The protocol used to induce LTD was low-frequency stimuli with a 200 ms paired pulse interval, 900 stimuli and a 1 Hz inter-pair interval. Paired-pulse facilitation was assessed via systematic stimuli with different intervals (25, 50, 100, 200, 400 and 800 ms). The paired-pulse ratio was obtained by dividing

the rising slope of the second fEPSP by the rising slope of the first fEPSP. Each experiment was performed on a slice from a different mouse. The recordings were made using MultiClamp 700B amplifiers. Data acquisition and analysis were performed using digitizer Digidata 1440A and analysis software pClamp 10 (Molecular Devices). Signals were filtered at 2 kHz and sampled at 10 kHz. All recordings were performed at 30°C by using an automatic temperature controller (Warner Instrument, Hamden, CT). Data are shown as mean ± standard error of mean. fEPSP slope was normalized to the baseline. LTP and LTD (%) were calculated as follows: $100 \times$ [mean fEPSP slope during the final 10 min of recording/mean baseline fEPSP slope]. Results were considered to be significant at $P < 0.05$.

RNA-sequencing and bioinformatics analysis

Three-month-old *Nr2f1*$^{+/-}$ or wild-type littermates were sacrificed. Total RNA was extracted from hippocampus using miRNeasy mini kit (Qiagen) with on-column DNase digestion according to the manufacturer's instructions. Pair-end RNA-Seq was performed using Illumina HiSeq 2500. Sequencing of all the samples was performed by the Genomic and RNA Profiling Core at Baylor College of Medicine. For each sample, about 40 to 60 million of 101 bp paired-end reads were generated. The quality of raw reads was assessed using FastQC. The average per base quality score across all the files was >34 and had passed all the major tests. The raw reads were aligned to the *Mus musculus* genome (Gencode Version M1—Ensembl 65/NCBIM37) using STAR v2.4.2a (40). The mappability of unique reads for each sample was above 89%. The htseq-count function in HTSeq (41) with union mode (–m union) was used to accumulate the number of aligned reads that falls under the exons of the gene. The obtained read counts are analogous to the expression level of each gene across all the samples. Genes with raw mean reads >10 (i.e. ~17 800 genes) were used for further downstream analysis. Normalization and differential gene expression analysis were carried out using the DESeq2 package (42) in R. The Wald test defined in the DESeq function of the package was used for differential expression analysis. A gene is called differentially expressed if the Benjamini-Hochberg false discovery rate (FDR) is <0.05, giving us a total of 1153 differentially expressed genes. Principal component analysis (PCA), hierarchical clustering plots (hclust) and XY plots between replicates of similar genotypes were used to do a sanity check for a nominal amount of non-technical variation and other latent factors. PCA and hclust plots were generated using ggplot2 (43). All the heatmaps of differentially expressed genes were generated using pheatmap package in R environment.

Quantitative real-time polymerase chain reaction

Total RNA was extracted from the mouse hippocampus with an miRNeasy Mini Kit (Qiagen) following the manufacturer's instructions. RNA was quantified using a NanoDrop 1000 spectrophotometer (Thermo Fisher). RNA was reverse-transcribed to complementary DNA using a reverse transcription kit (Qiagen). Complementary DNA samples then underwent quantitative real-time polymerase chain reaction on the CFX96 Touch Real-Time PCR Detection System (Bio-Rad Laboratories) with SYBR Green FastMix (Quanta Biosciences). Relative quantities of *NR2F1* messenger RNA were measured with the ΔΔCT method and normalized against the housekeeping gene *GAPDH*. The primer sequences were as follows: mouse *Nr2f1* forward, 5′-GCACTACGGCCAATTCACCT-3′; mouse *Nr2f1* reverse, 5′-TTGGAGGCATTCTTCCTCGC-3′; mouse *Mmp2* forward, 5′-GGACAAGTGGTCCGCGTAAA-3′; mouse *Mmp2* reverse, 5′-CCGACCGTTGAACAGGAAGG-3′; mouse *Mmp14* forward, 5′-CAGTATGGCTACCTACCTCCAG-3′; mouse *Mmp14* reverse, 5′-GCCTTGCCTGTCACTTGTAAA-3′; mouse *Mmp15* forward, 5′-CAGGAAAGGCATGGAACAAT-3′; mouse *Mmp15* reverse, 5′-TACCAGCCCAGCTTCTCAGT-3′; mouse *Hspg2* forward, 5′-TTCCAGATGGTCTATTTCCGGG-3′; and mouse *Hspg2* reverse, 5′-CTTGGCACTTGCATCCTCC-3′.

Supplementary Material

Supplementary Material is available at *HMG* online.

Acknowledgements

We thank the Small Animal MRI at Baylor College of Medicine and the Small Animal Imaging Facility (SAIF) at Texas Children's Hospital for MR imaging services. C.P.S. was generously supported by the Joan and Stanford Alexander Family.

Conflict of Interest statement. The authors declare no competing interests.

Funding

Weatherstone pre-doctoral fellowship from Autism Speaks (9120 to L.W.); BCM Intellectual and Developmental Disabilities Research Center and Neurobehavioral Cores (National Institutes of Health grant U54HD083092).

References

1. Bosch, D.G., Boonstra, F.N., Gonzaga-Jauregui, C., Xu, M., de Ligt, J., Jhangiani, S., Wiszniewski, W., Muzny, D.M., Yntema, H.G., Pfundt, R. *et al.* (2014) NR2F1 mutations cause optic atrophy with intellectual disability. *Am. J. Hum. Genet.*, **94**, 303–309.
2. Hino-Fukuyo, N., Kikuchi, A., Yokoyama, H., Iinuma, K., Hirose, M., Haginoya, K., Niihori, T., Nakayama, K., Aoki, Y. and Kure, S. (2017) Long-term outcome of a 26-year-old woman with West syndrome and an nuclear receptor subfamily 2 group F member 1 gene (NR2F1) mutation. *Seizure*, **50**, 144–146.
3. Chen, C.A., Bosch, D.G., Cho, M.T., Rosenfeld, J.A., Shinawi, M., Lewis, R.A., Mann, J., Jayakar, P., Payne, K., Walsh, L. *et al.* (2016) The expanding clinical phenotype of Bosch-Boonstra-Schaaf optic atrophy syndrome: 20 new cases and possible genotype-phenotype correlations. *Genet. Med.*, **18**, 1143–1150.
4. Martin-Hernandez, E., Rodriguez-Garcia, M.E., Chen, C.A., Cotrina-Vinagre, F.J., Carnicero-Rodriguez, P., Bellusci, M., Schaaf, C.P. and Martinez-Azorin, F. (2018) Mitochondrial involvement in a Bosch-Boonstra-Schaaf optic atrophy syndrome patient with a novel de novo NR2F1 gene mutation. *J. Hum. Genet.*, **63**, 525–528.
5. Kaiwar, C., Zimmermann, M.T., Ferber, M.J., Niu, Z., Urrutia, R.A., Klee, E.W. and Babovic-Vuksanovic, D. (2017) Novel NR2F1 variants likely disrupt DNA binding: molecular modeling in two cases, review of published cases, genotype-phenotype correlation, and phenotypic expansion of the Bosch-Boonstra-Schaaf optic atrophy syndrome. *Cold Spring Harb Mol Case Study.*, **3**.

6. Armentano, M., Chou, S.J., Tomassy, G.S., Leingartner, A., O'Leary, D.D. and Studer, M. (2007) COUP-TFI regulates the balance of cortical patterning between frontal/motor and sensory areas. *Nat. Neurosci.*, **10**, 1277–1286.
7. Tang, K., Xie, X., Park, J.I., Jamrich, M., Tsai, S. and Tsai, M.J. (2010) COUP-TFs regulate eye development by controlling factors essential for optic vesicle morphogenesis. *Development*, **137**, 725–734.
8. Bertacchi, M., Gruart, A., Kaimakis, P., Allet, C., Serra, L., Giacobini, P., Delgado-Garcia, J.M., Bovolenta, P. and Studer, M. (2019) Mouse Nr2f1 haploinsufficiency unveils new pathological mechanisms of a human optic atrophy syndrome. *EMBO Mol. Med*, in press, e10291.
9. Parisot, J., Flore, G., Bertacchi, M. and Studer, M. (2017) COUP-TFI mitotically regulates production and migration of dentate granule cells and modulates hippocampal Cxcr4 expression. *Development*, **144**, 2045–2058.
10. Qiu, Y., Pereira, F.A., DeMayo, F.J., Lydon, J.P., Tsai, S.Y. and Tsai, M.J. (1997) Null mutation of mCOUP-TFI results in defects in morphogenesis of the glossopharyngeal ganglion, axonal projection, and arborization. *Genes Dev.*, **11**, 1925–1937.
11. Cowan, C.S., Abd-El-Barr, M., van der, M., Lo, E.M., Paul, D., Bramblett, D.E., Lem, J., Simons, D.L. and Wu, S.M. (2016) Connexin 36 and rod bipolar cell independent rod pathways drive retinal ganglion cells and optokinetic reflexes. *Vision Res.*, **119**, 99–109.
12. van der Heijden, M.E., Shah, P., Cowan, C.S., Yang, Z., Wu, S.M. and Frankfort, B.J. (2016) Effects of chronic and acute intraocular pressure elevation on Scotopic and Photopic contrast sensitivity in mice. *Invest. Ophthalmol. Vis. Sci.*, **57**, 3077–3087.
13. Cai, T., Seymour, M.L., Zhang, H., Pereira, F.A. and Groves, A.K. (2013) Conditional deletion of Atoh1 reveals distinct critical periods for survival and function of hair cells in the organ of Corti. *J. Neurosci.*, **33**, 10110–10122.
14. Lone, A.M., Leidl, M., McFedries, A.K., Horner, J.W., Creemers, J. and Saghatelian, A. (2014) Deletion of PREPl causes growth impairment and hypotonia in mice. *PLoS One*, **9**, e89160.
15. Mikulecka, A. and Mares, P. (2002) NMDA receptor antagonists impair motor performance in immature rats. *Psychopharmacology (Berl)*, **162**, 364–372.
16. Hashemi, E., Sahbaie, P., Davies, M.F., Clark, J.D. and DeLorey, T.M. (2007) Gabrb3 gene deficient mice exhibit increased risk assessment behavior, hypotonia and expansion of the plexus of locus coeruleus dendrites. *Brain Res.*, **1129**, 191–199.
17. Luscher, C. and Malenka, R.C. (2012) NMDA receptor-dependent long-term potentiation and long-term depression (LTP/LTD). *Cold Spring Harb. Perspect. Biol.*, **4**.
18. Verslegers, M., Lemmens, K., Van Hove, I. and Moons, L. (2013) Matrix metalloproteinase-2 and -9 as promising benefactors in development, plasticity and repair of the nervous system. *Prog. Neurobiol.*, **105**, 60–78.
19. Pohodich, A.E., Yalamanchili, H., Raman, A.T., Wan, Y.W., Gundry, M., Hao, S., Jin, H., Tang, J., Liu, Z. and Zoghbi, H.Y. (2018) Forniceal deep brain stimulation induces gene expression and splicing changes that promote neurogenesis and plasticity. *Elife*, **7**.
20. Heckers, S. (2001) Neuroimaging studies of the hippocampus in schizophrenia. *Hippocampus*, **11**, 520–528.
21. Smith, M.E. (2005) Bilateral hippocampal volume reduction in adults with post-traumatic stress disorder: a meta-analysis of structural MRI studies. *Hippocampus*, **15**, 798–807.
22. Videbech, P. and Ravnkilde, B. (2004) Hippocampal volume and depression: a meta-analysis of MRI studies. *Am. J. Psychiatry*, **161**, 1957–1966.
23. Pinter, J.D., Brown, W.E., Eliez, S., Schmitt, J.E., Capone, G.T. and Reiss, A.L. (2001) Amygdala and hippocampal volumes in children with down syndrome: a high-resolution MRI study. *Neurology*, **56**, 972–974.
24. Deboer, T., Wu, Z., Lee, A. and Simon, T.J. (2007) Hippocampal volume reduction in children with chromosome 22q11.2 deletion syndrome is associated with cognitive impairment. *Behav. Brain Funct.*, **3**, 54.
25. Flore, G., Di Ruberto, G., Parisot, J., Sannino, S., Russo, F., Illingworth, E.A., Studer, M. and De Leonibus, E. (2017) Gradient COUP-TFI expression is required for functional Organization of the Hippocampal Septo-Temporal Longitudinal Axis. *Cereb. Cortex*, **27**, 1629–1643.
26. Debbane, M., Schaer, M., Farhoumand, R., Glaser, B. and Eliez, S. (2006) Hippocampal volume reduction in 22q11.2 deletion syndrome. *Neuropsychologia*, **44**, 2360–2365.
27. Collingridge, G.L., Peineau, S., Howland, J.G. and Wang, Y.T. (2010) Long-term depression in the CNS. *Nat. Rev. Neurosci.*, **11**, 459–473.
28. Ryu, J., Futai, K., Feliu, M., Weinberg, R. and Sheng, M. (2008) Constitutively active Rap2 transgenic mice display fewer dendritic spines, reduced extracellular signal-regulated kinase signaling, enhanced long-term depression, and impaired spatial learning and fear extinction. *J. Neurosci.*, **28**, 8178–8188.
29. Morice, E., Billard, J.M., Denis, C., Mathieu, F., Betancur, C., Epelbaum, J., Giros, B. and Nosten-Bertrand, M. (2007) Parallel loss of hippocampal LTD and cognitive flexibility in a genetic model of hyperdopaminergia. *Neuropsychopharmacology*, **32**, 2108–2116.
30. Cahill, H. and Nathans, J. (2008) The optokinetic reflex as a tool for quantitative analyses of nervous system function in mice: application to genetic and drug-induced variation. *PLoS One*, **3**, e2055.
31. Contesse, T., Ayrault, M., Mantegazza, M., Studer, M. and Deschaux, O. (2019) Hyperactive and anxiolytic-like behaviors result from loss of COUP-TFI/Nr2f1 in the mouse cortex. *Genes Brain Behav*, in press, e12556.
32. Kaiwar, C., Zimmerman, M.T., Ferber, M.J., Niu, Z., Urrutia, R.A., Klee, E.W. and Babovic-Vuksanovic, D. (2017) *Novel NR2F1 variants likely disrupt DNA binding: Molecular modeling in two cases, Review of Published Cases, Genotype-Phenotype Correlation and Phenotypic Expansion of the Bosch-Boonstra-Schaaf Optic Atrophy Syndrome*. Cold Spring Harb. Mol, Case Stud, in press.
33. Yonehara, K., Fiscella, M., Drinnenberg, A., Esposti, F., Trenholm, S., Krol, J., Franke, F., Scherf, B.G., Kusnyerik, A., Muller, J. *et al.* (2016) Congenital nystagmus gene FRMD7 is necessary for establishing a neuronal circuit asymmetry for direction selectivity. *Neuron*, **89**, 177–193.
34. Tabata, H., Shimizu, N., Wada, Y., Miura, K. and Kawano, K. (2010) Initiation of the optokinetic response (OKR) in mice. *J. Vis.*, **10**(13), 11–17.
35. Xia, A., Song, Y., Wang, R., Gao, S.S., Clifton, W., Raphael, P., Chao, S.I., Pereira, F.A., Groves, A.K. and Oghalai, J.S. (2013) Prestin regulation and function in residual outer hair cells after noise-induced hearing loss. *PLoS One*, **8**, e82602.
36. Hao, S., Tang, B., Wu, Z., Ure, K., Sun, Y., Tao, H., Gao, Y., Patel, A.J., Curry, D.J., Samaco, R.C. *et al.* (2015) Forniceal deep brain

stimulation rescues hippocampal memory in Rett syndrome mice. *Nature*, **526**, 430–434.
37. Zeitlin, R., Patel, S., Solomon, R., Tran, J., Weeber, E.J. and Echeverria, V. (2012) Cotinine enhances the extinction of contextual fear memory and reduces anxiety after fear conditioning. *Behav. Brain Res.*, **228**, 284–293.
38. Wolf, A., Bauer, B., Abner, E.L., Ashkenazy-Frolinger, T. and Hartz, A.M. (2016) A comprehensive behavioral test battery to assess learning and memory in 129S6/Tg2576 mice. *PLoS One*, **11**, e0147733.
39. Hsiao, K.K., Borchelt, D.R., Olson, K., Johannsdottir, R., Kitt, C., Yunis, W., Xu, S., Eckman, C., Younkin, S., Price, D. *et al.* (1995) Age-related CNS disorder and early death in transgenic FVB/N mice overexpressing Alzheimer amyloid precursor proteins. *Neuron*, **15**, 1203–1218.
40. Dobin, A., Davis, C.A., Schlesinger, F., Drenkow, J., Zaleski, C., Jha, S., Batut, P., Chaisson, M. and Gingeras, T.R. (2013) STAR: ultrafast universal RNA-seq aligner. *Bioinformatics*, **29**, 15–21.
41. Anders, S., Pyl, P.T. and Huber, W. (2015) HTSeq–a python framework to work with high-throughput sequencing data. *Bioinformatics*, **31**, 166–169.
42. Love, M.I., Huber, W. and Anders, S. (2014) Moderated estimation of fold change and dispersion for RNA-seq data with DESeq2. *Genome Biol.*, **15**, 550.
43. Wickham, H. and SpringerLink (Online service). In Use R!, in press., pp. XVI, 260 p. 232 illus., 140 illus. in color.